PHYSICAL REVIEW A VOLUME 18, NUMBER 6 DECEMBER 1978

Optical rotary saturation in a gas

Yehiam Prior,* J.A. Kash, and E. L. Hahn
Department of Physics, University of California, Berkeley, California 94720
(Received 31 July 1978)

The optical analog of the nuclear magnetic resonance rotary saturation effect is demonstrated and analyzed. A 9.6-μm CO_2 laser resonance excitation of vibrational transitions in gaseous CH_3F creates an effective splitting in the interaction representation of the optical two-level system. A radio-frequency standing-wave Stark electric field is tuned in rotary saturation resonance with the splitting. The change in transmitted laser beam intensity, because of rotary resonance, is measured in terms of transient optical signals obtained by the Stark switching method of Brewer and Shoemaker. The measured single and multiphoton rotary saturation resonance signals are compared with perturbation and computer solutions of nonlinear Bloch-Maxwell macroscopic equations. Doppler-free rotary saturation spectra are obtained in the presence of inhomogeneous Doppler broadening by a special scheme of Fourier analysis. A discussion is presented of the coupling of energy between two traveling waves that are in double resonance with the optical two-level system. The concept of spin temperature is discussed in relation to a coherently excited optical level system with a long fluorescence lifetime. The possibility of a cross-relaxation double resonance experiment between an optical system and a spin system is outlined.

I. INTRODUCTION

It is well known that a system with discrete quantum levels subjected to strong coherent resonance radiation can be described by an effective Hamiltonian that differs from the original unperturbed Hamiltonian in the absence of radiation. If a second weak probe field in a double-resonance experiment simultaneously inspects the resonance susceptibility of the modified system, the probe resonance response will show additional level splittings (not removal of degeneracies) or frequency shifts that depend upon the power and tuning of the strong field. Effects of this type (not necessarily involving double resonance) are the Bloch-Siegert,[1] Autler-Townes,[2] and alternating current (AC) Stark shift[3] effects. In an early NMR experiment in a liquid, Anderson[4] demonstrated very clearly the Rabi frequency shifted sidebands induced in a two-level system by a strong driving field. To account for the effects of strong NMR rf irradiation in solids Redfield[5] devised a spin temperature picture in which separate dipolar and Zeeman energy reservoirs in the same crystal could be defined at different spin temperatures simultaneously. In this picture effective splittings and population differences in the new interaction representation correspond to different spin temperatures for any given pair of spin levels. If the level splittings of two different spin reservoir species are made to coincide,[6] double resonance dipole-dipole coupling takes place, and the two spin reservoirs are viewed as arriving at a common spin temperature equilibrium. Alternatively, a particular reservoir may be subjected to a properly aligned external oscillating magnetic field applied at low frequency corresponding to the level splitting induced by the strong coherent radiation. In this case, transitions are induced between the two levels of the system while it is subjected to the strong field. The reduction of the two-level population difference because of the second low-frequency resonance in the rotating frame labels this effect as "rotary saturation."[5]

In this investigation we obtain the optical analog of the NMR rotary saturation effect.[7] By means of a double resonance technique, an ensemble of electric dipole moments is brought into interaction simultaneously with two oscillating electric fields at widely disparate frequencies. The intense field from a 9.6μ CO_2 propagating laser beam excites two-level vibrational transitions at or near resonance in gaseous $^{13}CH_3F$. This two-level laser excitation gives rise to a much lower two-level splitting in the megacycle range. At the same time a standing wave electric field excitation of Stark plates in the gas cell at the rotary resonance frequency causes saturation of the coherent polarization induced by the laser beam in the laboratory frame. The rotary resonance response is measured in terms of the change in coherent transient signals at 9.6μ emitted by the sample after the double resonance excitation is suddenly switched off.

Our quantitative analysis of the rotary saturation experiment is based upon the optical two quantum level analog[8] of NMR spin dynamics, requiring the solution of modified Bloch-type equations. As a qualitative illustration of the effect, the schematic energy level diagram of Fig. 1 is very helpful. The rotary saturation experiment involves a probe excitation of the smaller direct splitting

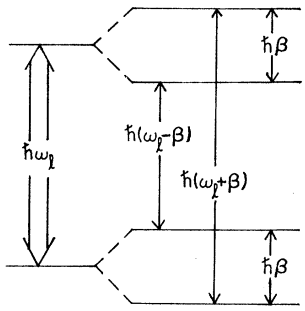

FIG. 1. Spectroscopy of a two-level system in the presence of intense coherent resonance radiation at frequency ω_l. As shown on the right, the effective Hamiltonian of the two-level system in the presence of resonance radiation at $\hbar\omega_l$ presents four eigenlevels. Rotary resonance saturation pertains to transitions at the induced splitting $\hbar\beta$. Transitions of the type $\hbar(\omega_l \pm \beta)$ were first observed in NMR also.

in the rotating frame of reference, in our case by a standing wave, although a probe rotary resonance traveling wave could be applied instead. Because of the saturation effect of the strong laser beam, the apparent probe resonance susceptibility is conditioned to be correspondingly negative or positive, depending upon which side of the laboratory frame transition frequency the strong laser excitation is applied. In other words, when the two level system appears to have its population inverted with respect to an effective field in the rotating frame, the system acts as an amplifier for the probe beam, although in fact the two-level population is not inverted in the laboratory frame. This interesting effect introduces a new optical susceptibility mechanism by which two fields of coherent radiation at different frequencies may couple to one other by means of nonlinear resonant coupling to a single two-level atomic system. Thus the rotary double resonance principle is similar to the two-level system double resonance effect of two laser beams in the laboratory frame, one an intense beam and the other a weak probe beam, tuned within a linewidth of one another.[9] This similarity will be discussed later.

As was mentioned above, the treatment of optical rotary saturation in a gas requires the solution of a nonlinear set of modified Bloch equations[7] applicable as well to NMR rotary saturation in liquids, where the dipole-dipole-coupling energy reservoir does not exist. These equations differ from the Bloch equations because of additional time-dependent terms which account for the probe field modulation. Since no closed-form analytic solution exists, a perturbation expansion approach is used, resulting in solutions applicable under conditions to be outlined later. In fact, the solution applies to the general resonance response of a two-level system line during magnetic or Stark modulation, traditional in measuring lineshapes in the regime where the modulation frequency Ω is slow compared to the inverse time width T_2^{-1}. For the condition $\Omega \sim 1/T_2$, faithful lineshape modulation response no longer is displayed, so that a type of "Debye resonance" response of the system polarization is predicted in the rotating frame. For values of Ω in excess of T_2^{-1}, comparable to effective Hamiltonian frequencies in the rotating frame, and for weak modulation amplitudes, single photon rotary resonance occurs. As the probe field intensity is increased, multiphoton resonances appear[10] and the system can no longer be described by the simple level diagram of Fig. 1.

It should be noted that the analog of NMR "spin temperature" equilibrium in solids does not generally carry over into the optical case. A single species optical dipolar energy reservoir probably cannot be realized. In a solid, electric dipole-dipole interaction energy is not readily conserved within an isolated two-level ensemble of dipoles, which prevents the onset of a quasi-equilibrium temperature different from the lattice temperature. Naturally, such an equilibrium would be possible if the isolated system energy would remain intact for times long compared to the formally estimated dipole-dipole coupling time, designated as T_2. For optical dipoles this equilibrium is not favored due to rapid spontaneous emission or strong coupling to broad collisional phonon degrees of freedom, which introduce competitive lifetimes comparable to or shorter than the optical system electric dipole-dipole coupling time. However, a very dilute system of optical dipoles may be assigned a temperature if it is prepared in such a way that it interacts exclusively, for example, by resonance coupling with an abundant species of spins, where the spins are in dipolar thermal equilibrium contact among themselves. A temperature may therefore be assigned to the dilute optical dipoles even though they do not couple directly among themselves. As pointed out in a later discussion, this would require a doped constituent in a solid with a forbidden transition that provides a long fluorescence lifetime.

II. OPTICAL ROTARY RESONANCE ANALYSIS

Consider a two-level system irradiated by a laser field $E_x(z,t)$ linearly polarized in the x direction and propagating as a plane wave in the z direction:

$$E_x(z,t) = \mathcal{E}_l \cos(\omega_l t - kz) . \quad (1)$$

$\mathcal{E}_l$ is the laser amplitude modulus, ω_l is the laser frequency, and $k = 2\pi/\lambda$, where λ is the wavelength. The standing wave Stark rotary saturation field

$$E_a(t) = \mathcal{E}_a \cos\Omega t \tag{2}$$

is applied parallel to $E_x(z,t)$ by means of a pair of Stark plates aligned parallel to the z direction in the gas cell. The function of $E_a(t)$ is to modulate the energy level spacing. The field E_a could as well be a traveling wave. For a particular rotational angular momentum quantum number M_J assigned to a pair of eigenlevels, a vibrational transition frequency $\omega_0 \sim \omega_l$ for $\Delta M_J = 0$ in gaseous $^{13}CH_3F$ is sinusoidally modulated at the low frequency Ω. The maximum linear Stark shift in energy splitting away from $\hbar\omega_0$ is given by

$$2\hbar\omega_a = A(M_J)\mathcal{E}_a . \tag{3}$$

The linear Stark shift constant $A(M_J)$ for a particular M_J relates the shift in vibrational eigenlevel energy to the applied Stark electric field. This constant applies as well for Stark pulse switching of levels into and out of resonance, a technique of Brewer and Shoemaker,[11] which we apply in order to observe free induction signal transients that give a measure of the rotary resonance effect. With the conditions $\kappa\mathcal{E}_l$, ω_a, $\Omega \ll \omega_l$, a two-level Hamiltonian can be defined

$$\mathcal{H} = \mathcal{H}_0[1 + (2\omega_a/\omega_0)\cos\Omega t] - p_x E_x(z,t) , \tag{4}$$

where $\kappa = 2p_0/\hbar$ and p_0 is the dipole transition matrix element. The matrix for the doubly perturbed system in the interaction representation for rotary saturation is therefore

$$\mathcal{H}_R = -\hbar \begin{pmatrix} \frac{1}{2}(\omega_0 - \omega_l) + \omega_a \cos\Omega t & \kappa\mathcal{E}_l \\ \kappa\mathcal{E}_l & -\frac{1}{2}(\omega_0 - \omega_l) - \omega_a \cos\Omega t \end{pmatrix}, \tag{5}$$

where

$$\mathcal{H}_R = \exp[i(\mathcal{H}_0/\hbar\omega_0)\omega_l t]\mathcal{H}\exp[-i(\mathcal{H}_0/\hbar\omega_0)\omega_l t] .$$

In general, ω_a may obtain from any diagonal susceptibility (Zeeman, Stark, or acoustic); but if there is no such susceptibility, the equivalent effect of Eq. (4) may be obtained by subjecting the laser to phase modulation so that

$$\omega_l t \rightarrow \omega_l t + (2\omega_a/\Omega)\sin\Omega t .$$

This phase modulation will result in the same Hamiltonian matrix $\mathcal{H}_R$ given by Eq. (5).

The coupled optical Bloch-Maxwell equations well known in the literature[12] form the basis for analysis of the optical rotary resonance experiment. The Bloch equations for polarization source terms with inclusion of rotary perturbation[7] follow directly from the Liouville equation for the density matrix ρ (with addition of T_1, T_2-type damping terms)

$$\begin{aligned} \dot{u} &= (\Delta\omega_l + 2\omega_a\cos\Omega t)v - u/T_2 , \\ \dot{v} &= -(\Delta\omega_l + 2\omega_a\cos\Omega t)u + \kappa\mathcal{E}_l w - v/T_2 , \\ \dot{w} &= -\kappa\mathcal{E}_l v - (w - w_0)/T_1 . \end{aligned} \tag{6}$$

The radiating source polarization[13]

$$P = Np_0(u + iv) \tag{7}$$

is coupled to the energy density

$$Nw(\tfrac{1}{2}\hbar\omega_0) = W = N\,\mathrm{Tr}(\mathcal{H}_0\rho) \tag{8}$$

of the two-level system, where N is the number density of two-level atoms, and

$$\begin{aligned} u &= \rho_{12} + \rho_{21} , \\ v &= -i(\rho_{12} - \rho_{21}) , \\ w &= \rho_{22} - \rho_{11} . \end{aligned} \tag{9}$$

For the two-level system defined by 1:ground state, 2:excited state, the complete ground state occupation gives $w_0 = -1$, and $W_0 = -\frac{1}{2}N\hbar\omega_0$. The off-resonance parameter

$$\omega_0 - \omega_l = \Delta\omega_l \tag{10}$$

will pertain to packets of dipoles off resonance with respect to the laser frequency applied within the Doppler spectrum of gaseous CH_3F.

The experimental procedure for obtaining and measuring optical rotary resonance in the presence of a broad Doppler spectrum employs a scheme of Fourier analysis. Doppler-free spectral information concerning more than one type of two-level transition with a specific matrix element can be obtained in the presence of an inhomogeneously broadened spectrum.[14] At a given applied rotary frequency Ω the steady-state rotary resonance is obtained while the laser two-level excitation is at equilibrium. A differential method of comparison (subtraction) of optical free induction signal amplitudes is first carried out. As shown in Fig. 2, a subtraction of successive free induction signals (FID) yields a differential signal $D(t)$ dependent only on rotary resonance because one signal depends on the past existence of rotary perturbation ($\omega_a \neq 0$), and the following subtracted signal does not ($\omega_a = 0$). Steady-state equilibrium resonance by the laser alone ($\omega_a = 0$)

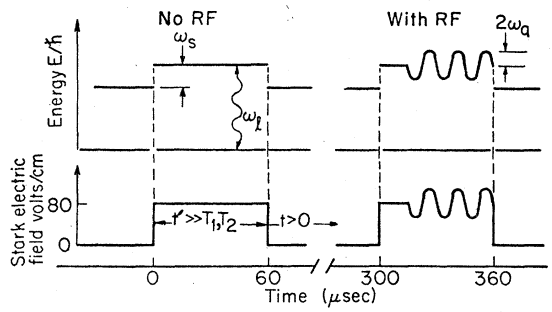

FIG. 2. Stark voltage sequence (below) and corresponding two-level energies (above). The differential signal caused by rf rotary saturation is obtained by subtracting the FID signal with no rf from the FID signal with rf. The 80 V/cm Stark pulse corresponds to $\omega_{s0}/2\pi = 3.55$ MHz.

is established in a time $t' \gg T_2$ before free precession is obtained. The equilibrium polarization $P_e(\omega_a = 0)$, which later yields the free precession signal, is obtained by setting $\dot{u} = \dot{v} = \dot{w} = 0$ in Eqs. (6). Therefore

$$P_e(\omega_a = 0) = Np_0(u_e + iv_e)\,, \tag{11}$$

where

$$u_e = [\,\Delta\omega_l\,\omega_1 T^2/(1+\beta^2 T^2)]w_0\,, \tag{12}$$

$$v_e = [\,\omega_1 T/(1+\beta^2 T^2)]\,w_0\,, \tag{13}$$

$$w_e = [\,1+\Delta\omega_l^2 T^2/(1+\beta^2 T^2)]w_0\,, \tag{14}$$

with $T_2 = T_1 = T$, $\omega_1 = \kappa\mathcal{E}_l$, and

$$\beta = (\Delta\omega_l^2 + \kappa^2\mathcal{E}_l^2)^{1/2}\,. \tag{15}$$

The polarization P_e radiates freely for the time $t \geq 0$ after a step-function Stark field E_x is switched on at $t = 0$. Dipole transitions initially tuned to $\omega_l \approx \omega_0$ are switched out of laser resonance to a new frequency $\omega_0 + \omega_s$, and the polarization P_e emits at that new frequency. The laser field $\mathcal{E}_l$ does not perturb the freely radiating P_e for the condition

$$\omega_s \gg T^{-1}[1 + (\kappa\mathcal{E}_l T)^2]^{1/2} = T'^{-1}\,, \tag{16}$$

where $1/T'$ is the excited spectral width. The Bloch equations (6) then apply for $\mathcal{E}_l = \omega_a = 0$ during $t \geq 0$. We specify that the laser is tuned near the center of the Doppler distribution, given by

$$g(\omega_0) = (2\pi\delta^2)^{-1/2}\exp[-(\omega_0 - \omega_{00})^2/2\delta^2]\,, \tag{17}$$

where $\omega_0 = \omega_{00} + kv$, with ω_{00} the two-level transition for the molecule at rest, and kv the Doppler frequency shift corresponding to molecular velocity v parallel to the z axis. Essentially, a flat distribution over the excited spectrum occurs since the Doppler width is large enough (~60 MHz for CH_3F) so that

$$\delta \gg \omega_s \gg T'^{-1}\,. \tag{18}$$

As a result, we set $g(\omega_0) \approx (2\pi\delta^2)^{-1/2}$.

The laser beam, which is always present, provides a heterodyne reference signal which beats with the radiated free precession dipole field at frequency ω_s. The optical-free precession signal[12] during $t \geq 0$ is measured in terms of a slowly varying field intensity $|E(t)^2|$ at the detector placed at the output from the gas sample

$$|E(t)^2|_{\omega_a=0} = \mathcal{E}_l^2 + \frac{4\sqrt{2\pi}\,\mathcal{E}_l\omega_l N p_0 L e^{-t/T}}{c\delta} \times \int_{-\infty}^{\infty} [u_e \sin(\Delta\omega_l + \omega_s)t + v_e \cos(\Delta\omega_l + \omega_s)t]d\Delta\omega_l\,. \tag{19}$$

A term proportional to $N^2 p_0^2$ in Eq. (19) is dropped as negligible.

The action of rotary saturation ($\omega_a \neq 0$) changes the laser-beam intensity $|E(t)^2|_{\omega_a=0}$ to a different value $|E(t)^2|_{\omega_a\neq 0}$. The rotary resonance solutions to the Bloch equations (6) in dynamic steady state obtain again for $t' \gg T_2$, but they do not derive simply from the condition $\dot{u} = \dot{v} = \dot{w} = 0$ which was applied when $\omega_a = 0$. The presence of the term $2\omega_a \cos\Omega t$ gives rise to steady-state oscillatory polarization components which oscillate at frequency Ω. No closed-form analytic general solutions exist for these equations. Exact solutions for $P_e(\omega_a \neq 0)$ must be obtained by numerical integration. Corrections to the unperturbed $P_e(\omega_a = 0)$ solution are obtained by a perturbation treatment presented in the Appendix for the condition $\omega_a/\kappa\mathcal{E}_l \ll 1$. We present the first-order perturbation results since they reveal the essential physical principles of rotary resonance. The full details of this calculation are given elsewhere.[15] For steady-state rotary perturbation, Eq. (11) may be rewritten

$$P_e(\omega_a \neq 0) = P_e(\omega_a = 0) + \Delta P = Np_0[u_e + \Delta u + i(v_e + \Delta v)]\,, \tag{20}$$

where $\Delta u = u_r + u_{ar}$ and $\Delta v = v_r + v_{ar}$. The first-order solution for the ΔP change has resonant (u_r, v_r) and antiresonant (u_{ar}, v_{ar}) parts. The antiresonant terms are obtained by $\Omega \to -\Omega$ substitution in the expressions below, where we express only the resonant terms

$$\Delta P_r(t') = Np_0(u_r + iv_r)\,.$$

In the rotating frame of reference these terms have driven rotary oscillatory character

$$u_r(t') = u_{c,r}\cos\Omega t' + u_{s,r}\sin\Omega t'$$
$$v_r(t') = v_{c,r}\cos\Omega t' + v_{s,r}\sin\Omega t'\,, \tag{21}$$

where the different times t' and t are defined in Fig. 2 and the coefficients are given by

$$u_{c,r} = \frac{\omega_a T v_e}{1+\Omega^2 T^2}\left[1+\Delta\omega_1^2 T^2 \frac{(\Omega T^2 + 2/\beta)(\Omega-\beta)}{1+(\Omega-\beta)^2 T^2}\right], \tag{22a}$$

$$u_{s,r} = \frac{\omega_a T v_e}{1+\Omega^2 T^2}\left[\Omega T + \Delta\omega_1^2 T \frac{\Omega T^2(\Omega/\beta - 3) + \beta T^2 - 1/\beta}{1+(\Omega-\beta)^2 T^2}\right], \tag{22b}$$

$$v_{c,r} = \frac{\omega_a \Delta\omega_1 T^2 v_e (\Omega/\beta - 2)}{1+(\Omega-\beta)^2 T^2}, \tag{22c}$$

and

$$v_{s,r} = -\frac{\omega_a \Delta\omega_1 T v_e [(\Omega-\beta)T^2 + 1/\beta]}{1+(\Omega-\beta)^2 T^2}. \tag{22d}$$

After a time $t' \gg T$ during which the above steady state is established, the Stark field step function E_s is switched off and initiates the free precession signal at a particular time defined as $t = 0$. The phase of the rf oscillation in Eqs. (21) must therefore be locked to the Stark pulse so that the pulse is always switched off at the same phase $\Omega t'$, where we chose $\cos\Omega t' = 0$ or 1.

The difference transient signal intensity caused by rotary saturation is

$$D(t) = |E(t)|^2_{\omega_a \neq 0} - |E(t)|^2_{\omega_a = 0}, \tag{23}$$

where $|E(t)^2|_{\omega_a \neq 0}$ is obtained by replacing u_e and v_e in Eq. (19) by $u_e + \Delta u$ and $v_e + \Delta v$, respectively. If a perturbation solution is desired, $D(t)$ is obtained directly by replacing u_e and v_e in Eq. (19) by the desired order of Δu and Δv, respectively. It should be noted that a nutation signal[11] is created from those transitions that are Stark switched into resonance with ω_l. This signal comes from molecules tuned to $\omega_0' = \omega_0 - \omega_s$ in the Doppler spectrum before E_s is switched. The differential signal method in our experiment cancels out the nutation signal since it occurs with equal amplitude after every switching of E_s.

The changed ($|E(t)|^2_{\omega_a \neq 0}$) and unchanged ($|E(t)|^2_{\omega_a = 0}$) FID signals are sampled and stored electronically. The differential signal $D(t)$ is amplified, averaged in a boxcar integrator, and finally Fourier-analyzed by a computer. The Fourier transform

$$S(\Omega, \Delta\omega_l) = \int_{-\infty}^{\infty} D(t) e^{i\omega t} dt \tag{24}$$

is obtained at a particular frequency $\omega = \omega_s + \Delta\omega_l$. The experiment is repeated for different values of Ω. The response $S(\Omega, \Delta\omega_l)$ ultimately may be plotted for all ranges of Ω and $\Delta\omega_l$.

A. Measurements of CH_3F

Our measurements apply to the case of vibrational transitions in $^{13}CH_3F$ which is 95% isotopically enriched in ^{13}C. The $(J, K) = (4, 3) \leftrightarrow (5, 3)$ rotational transition of the ν_3 fundamental vibrational mode is excited by the $P(32)$ CO_2 laser line at 9.66 μm. With the laser field E_l polarized parallel to E_s and E_a, there exist nine separate two-level transitions, independent of one another, defined by $\Delta M_J = 0$ with $M_J = 0, \pm1, \pm2, \pm3, \pm4$.

The step Stark field E_s provides equally spaced level separations where

$$\omega_s = M_J \omega_{s0} = E_s A(M_J)\hbar^{-1}, \tag{25}$$

similar to Eq. (3). Two sets of four spectral lines are obtained from the $\Delta M = 0$ transitions that are equally spaced by frequency ω_{s0}. Each set is symmetric about the $M = 0 \leftrightarrow M = 0$ transition. This transition by itself does not contribute to the data because it does not respond to a Stark field and cannot be probed by the Stark switching method. If $\omega_s = M_J \omega_{s0}$ is sufficiently different for each of the transitions, then each of the four lines can, in principle, be distinguished from one another in the Fourier analysis providing that the condition $\omega_{s0} \gg 1/T'$ [Eq. (16)] permits resolution of these lines.[14] In the measurement of multiphoton rotary saturation responses to be discussed later, ω_{s0} must be made even larger to prevent the multiple photon satellite lines of one M_J transition from overlapping with satellites from neighboring lines.

B. Multiphoton resonances

The obvious single photon optical rotary resonance occurs for $\Omega = \beta$, as seen in resonance denominators of Eqs. (22), for $\omega_a \ll \kappa\delta_l$. The first terms of Eqs. (22a) and (22b) provide a curious effect which would relate to observations in which the condition $\Omega \sim 1/T_2$ applies. Ordinarily, the lineshape modulation technique in conventional spectroscopy would require $\Omega \ll 1/T_2$. A violation of this condition would result in such terms, with $u_{c,r}$ absorptive and $u_{s,r}$ dispersive. These terms are of the same form as those obtained for Debye resonance of polar molecules. Here we have a type of "Debye resonance in the rotating frame," which refers to the extent to which the polarization can relax and follow $2\omega_a \cos\Omega t$ as it oscillates near $\Omega \sim 1/T$.

When higher rf power is applied (corresponding to at least 20 V/cm) so that $\omega_0/\kappa\delta_l \gtrsim \frac{1}{2}$, the designations of perturbation probe field and intense pump field are no longer meaningful. As a result, multiphoton rotary saturation transitions are obtained as pointed out in the Appendix. A second-order perturbation calculation predicts terms oscillating at 2Ω with resonant denominators of the form $1 + (\beta - 2\Omega)^2 T^2$, typical of a two-photon transition. For an n-photon transition

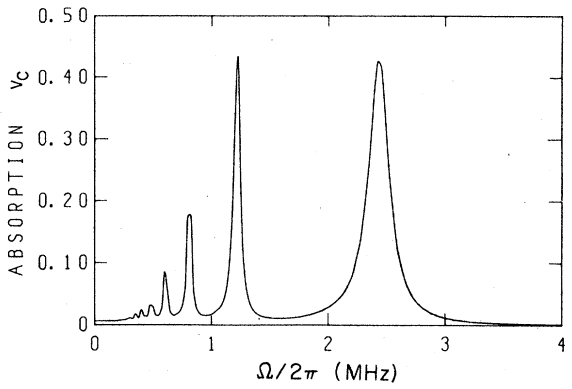

FIG. 3. Exact numerical solution for multiphoton rotary saturation resonances at $\Omega=\beta/n$. The plotted quantity $v_c=\Delta v=v-v_e$ is calculated in steady state with ending phase $\Omega t'=0$. Other parameters are $\Delta\omega_l=15$ rad/μsec, $\omega_a=\omega_1=3$ rad/μsec, and $T_1=T_2=3$ μsec. $w_0=1$ defines the normalization.

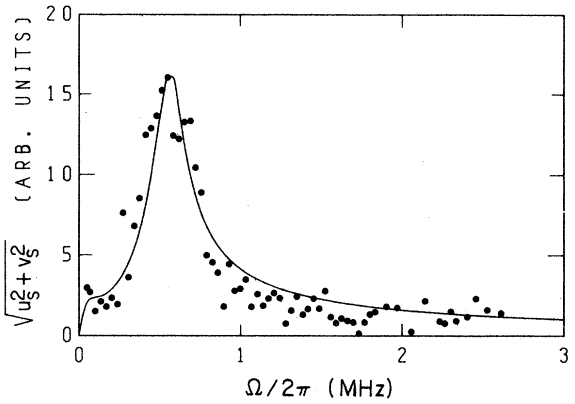

FIG. 4. Single photon rotary resonance response for $\Delta\omega_l=2.5$ rad/μsec, $\omega_1=3$ rad/μsec, $2\omega_a=0.5$ rad/μsec, and $\Omega t'=\frac{1}{2}\pi$ at rf turnoff. The solid curve is the perturbation solution $|S(\Omega,\Delta\omega_l)|=(u_S^2+v_S^2)^{1/2}$ fitted to $T=2.2$ μsec. $^{13}CH_3F$ pressure of 1 micron applies to all experimental results presented here.

in general we have the rotary resonance condition

$$\Omega=\beta/n\,. \tag{26}$$

The positions and widths of such transitions are shown in the computer plot of Fig. 3.

C. Experimental results

The technique of optical Stark switching by Brewer and Shoemaker[11] is adapted for the observation of optical rotary resonance. A principal experimental modification is the superposition of an oscillating field $E_a(t)$ upon the dc pedestal field E_S. Parallel Stark plates, consisting of aluminum coated on glass, are separated by rigid quartz supports and housed in a two-meter long cell. The laser beam traverses the length of the cell four times by three reflections from mirrors at each end of the cell. The intensity of the TEM_{00} mode Gaussian profile beam, with a 2 cm diameter, is about 0.25 watts/cm^2, giving a peak value of $\kappa\mathscr{E}_l/2\pi\sim 1$ MHz. Figure 4 compares the theoretical computer prediction plot for single-photon rotary resonance with experiment, with the condition $\omega_a\ll\kappa\mathscr{E}_l$. For a chosen value of $\Delta\omega_l$, only the Fourier transform magnitude $(u_S^2+v_S^2)^{1/2}=|S(\Omega,\Delta\omega_l)|$ is plotted versus Ω. From Eqs. (22) we define $u_s=u_{s,r}+u_{s,ar}$ and $v_s=v_{s,r}+v_{s,ar}$. This magnitude is chosen in order to avoid the experimental phase uncertainty which mixes the cosine and sine transform functions in Eq. (19). We display rotary resonance data for $\Delta\omega_l^2\gg\omega_1^2$. Under this condition $\beta\sim\Delta\omega_l$ and the rotary saturation difference transient signal $D(t)$ [Eq. (23)] will be affected mainly by those components of the spectrum which are far off resonance. Therefore it can be shown that the function $(u_S^2+v_S^2)^{1/2}$ obtained from the squares of the cosine and sine transforms, exhibited by the form of Eq. (19), is approximately valid if the effect of the decay factor $e^{-t/T}$ is included by redefining T as $\frac{1}{2}T$ in the Bloch equations. Thus we set $e^{-t/T}=1$ in Eqs. (19) and (23), since it will manifest itself instead in $S(\Omega,\Delta\omega_l)$ [Eq. (24)] (only for large $\Delta\omega_l$) in terms of the added linewidth. This approximation is well justified in the perturbation limit $\omega_a\ll\kappa\mathscr{E}_l,\kappa\mathscr{E}_l\ll\Delta\omega_l$, where the analysis presents a convolution of two Lorentzian functions of width T^{-1}. A resultant Lorentzian function is obtained of width $\frac{1}{2}T^{-1}$. For $\omega_a\sim\kappa\mathscr{E}_l$ the multiphoton resonance responses are shown in Fig. 5. All data is displayed for the $M_J=1\leftrightarrow M_J=1$ transition only. The values of Ω_{max} at which the resonance peaks occur, from the condition $\Omega=\beta/n$, are plotted

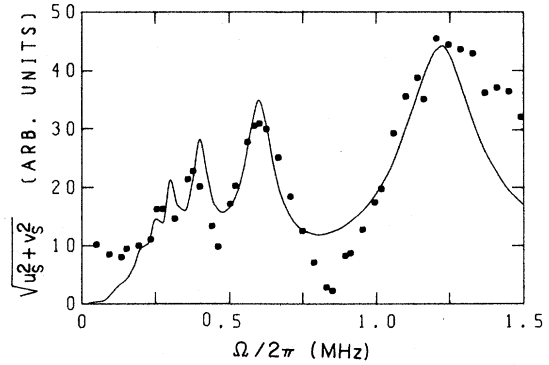

FIG. 5. Multiple photon resonance for $\Delta\omega_l=7.5$ rad/μsec, $\omega_1=1$ rad/μsec, $2\omega_a=4.6$ rad/μsec, with $\Omega t'=\frac{1}{2}\pi$ at rf turnoff. The solid curve is the numerical solution for $|S(\Omega,\Delta\omega_l)|=(u_S^2+v_S^2)^{1/2}$ to Eqs. (6) for the above parameters, with $T_1=T_2=2.2$ μsec.

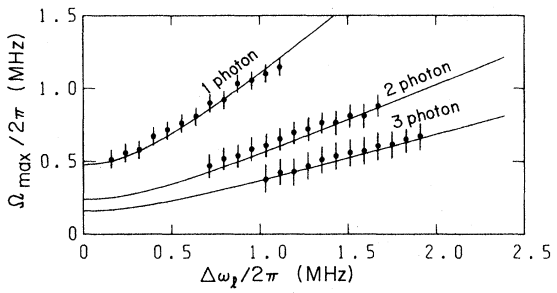

FIG. 6. Experimental rotary resonance maxima Ω_{max} for $n=1,2,3$ photon transitions vs $\Delta\omega_l$. The solid curves are plots of $\Omega_{max}=(\kappa^2\mathcal{E}_l^2+\Delta\omega_l^2)^{1/2}/n$, the rotary resonance relation, for $\kappa\mathcal{E}_l=3$ rad/μsec. The data was taken with $\Omega t'=0$ at rf turnoff, although data with $\Omega t'=\frac{1}{2}\pi$ at rf turnoff also fit the relation. The one photon curve has been verified out to $\Omega_{max}/2\pi=2.5$ MHz for low rf powers.

versus $\Delta\omega_l$ in Fig. 6. The error in the theory associated with the $\frac{1}{2}T$ ansatz above for $\omega_a\sim\kappa\mathcal{E}_l$ is less than the 10% to 15% error contributed by a number of experimental conditions to be outlined below. The validity of the effective $\frac{1}{2}T=T_e$ relaxation time definition is borne out by a fit of the one-photon and multiphoton rotary resonance curves to a relaxation time of $T_e=2.2$ μsec, which corresponds well within experimental error to a measured photon echo envelope lifetime[14] of T_2 ~ 5 μsec for the $M_J=1\leftrightarrow 1$ transition at a CH_3F pressure of 1 micron.

As our data points pertain mostly to the condition $(\Delta\omega_l)^2\gg(\kappa\mathcal{E}_l)^2$ for two sets of four spectral lines symmetric about the $M_J=0\leftrightarrow 0$ transition, the rotary resonance maxima occur essentially at the same $\Omega\approx\Delta\omega_l$. We emphasize that since $\omega_S=M_J\omega_{s0}$ is different for each transition $M_J\leftrightarrow M_J$ ($|M_J|=1$, 2, 3, 4), each of the four lines in the Fourier analysis can be distinguished from one another in their response to rotary resonance. When multiphoton satellite lines appear for higher rf power ($E_a\gtrsim 20$ V/cm), the Stark field E_s and the corresponding ω_{s0} parameter must be increased to avoid overlap of satellite resonances from neighboring M_J lines. This problem is avoided in our experiment by analyzing the $M_J=1$ rotary resonance multiphoton lines for negative $|\Delta\omega_l|$, thus avoiding the satellite resonances from the $M_J=2$ transition on the other side ($+|\Delta\omega_l|$) of the $M_J=1$ line.[16]

From Eq. (3) the parameter $A(M_J)=0.044\,M_J$ (MHz/volt-cm^{-1}) in practical units applies to CH_3F. A Stark field $E_S=80$ volts/cm corresponds to $\omega_{s0}=\omega_s=22.3\times10^6$ rad-sec^{-1} for the $M_J=1$ transition. Initial phase uncertainty in Eq. (19) and a smaller signal amplitude reduction in transient signals due to a slight amount of adiabatic following is caused by the finite Stark voltage turnoff time $t_f\sim 50$ ns. The effect of resultant phase uncertainty of $\omega_s t\sim 1$ rad is avoided by use of the phase independent $(u_S^2+v_S^2)^{1/2}$ in plotting data. The finite turnoff time also causes a slight violation of the adiabatic condition (in the rotating frame),

$$\frac{d\omega_s}{dt}\gg\frac{\beta^3}{\omega_1},$$

producing a signal amplitude change of a few percent, as borne out by computer modelings. Other sources of experimental error are as follows: (i) Inhomogeneity of $\mathcal{E}_l$ over the laser Gaussian beam profile, laser beam divergence, beam losses due to mirror reflections, and beam overlap effects (Lamb-dip-type interactions) account for uncertainty in assignment of $\mathcal{E}_l$ as a parameter in the experiment. The values of $\mathcal{E}_l$ quoted in our data are averages deduced from data fitting, whereas an integral over a distribution of $\mathcal{E}_l$ values would be formally appropriate but impractical in view of all the experimental uncertainties in the final data. (ii) Power drifts from the CO_2 laser during the course of Fourier transform measurements affect the uncertainty in fitted values. Nevertheless, the values of $\mathcal{E}_l$ quoted are reasonably confirmed from measurements of optical nutation oscillation periods.[11] Laser frequency (ω_l) stability is necessary for only short times $t\sim T_2$. (iii) Errors occur in computer Fourier transform calculation resulting from finite cutoff in bandwidth of the Fourier analysis.

The above errors combine to contribute an estimate of about 15% spread in the amplitude of experimental rotary resonance plots. There remain, however, unexplained deviations from the predicted computer plot shapes for multiphoton behavior, as shown in Fig. 5. However, for n not exceeding 3 in Eq. (26), the multiphoton resonance frequencies Ω_{max} fall within experimental error, and we have not confirmed transitions for $n>3$.

III. RELATED APPLICATIONS

A. Double optical resonance coupling between traveling waves

The rotary saturation experiment may be thought of as a low-frequency resonance phenomenon which takes place in the frame of reference rotating at the high frequency of the laser. The laser is near resonance with the two-level system in the laboratory frame. If one applies a second traveling wave laser beam

$$E_2(z,t)=\mathcal{E}_2\cos[(\omega_l+\epsilon)t+k_2z],$$

in place of the low-frequency rotary perturbation field E_a, again a double resonance coupling effect

may be achieved[9] similar to rotary saturation. Let $\epsilon \ll \omega_l$ and $k_2 \approx k$. As ϵ varies, $\omega_l + \epsilon$ is scanned across the resonance line driven by the laser at frequency ω_l. In the frame of reference rotating at ω_l the laser field modulus $\mathcal{E}_l$ appears stationary, while the modulus $\mathcal{E}_2$ of the second laser appears to rotate at angular frequency $\pm\epsilon$ with respect to $\mathcal{E}_l$, depending on the applied frequency $\omega_l \pm \epsilon$. If the matching condition

$$\beta = (\Delta\omega_l^2 + \kappa^2 \mathcal{E}_l^2)^{1/2} = \epsilon$$

occurs, the rotation of $\mathcal{E}_2$ is synchronous with the rotation of the optical pseudopolarization vector $\bar{P}_T$ in the rotating frame, quite similar to the mechanism of rotary resonance. A component of $\bar{\mathcal{E}}_2$ perpendicular to $\bar{\beta}$ becomes effective in producing saturation of P_T, just as the component $(\omega_1/\Delta\omega_l)\mathcal{E}_a$ (for $\Delta\omega_l \gg \omega_1$) is effective in causing rotary saturation of P as seen by inspection of Eqs. (22). Stimulated gain or loss of rotary field standing energy density (or flux for a traveling wave) depends upon the sign of $\Delta\omega_l$ in $v_{c,r}$ (i.e., let $\beta = \Omega$), showing that gain is obtained if P corresponds to an inverted amplifying two level system for $-|\Delta\omega_l|$, and an absorber for $+|\Delta\omega_l|$. These cases are shown schematically in Fig. 7.

With the definitions $\omega_2 = \kappa\mathcal{E}_2$ and ξ an arbitrary phase angle between two coupled traveling waves (which must remain constant for a relaxation time of order T_1), the Bloch-type equations analogous to Eqs. (6) are easily shown (from the classical torque equation) to be

$$\begin{aligned}
\dot{u} &= \Delta\omega_l v - \omega_2 \sin(\epsilon t + \xi) w - u/T_2 , \\
\dot{v} &= -\Delta\omega_l u + [\omega_1 + \omega_2 \cos(\epsilon t + \xi)] w - v/T_2 , \\
\dot{w} &= \omega_2 \sin(\epsilon t + \xi) u \\
&\quad - [\omega_1 + \omega_2 \cos(\epsilon t + \xi)] v - (w - w_0)/T_1 .
\end{aligned} \tag{27}$$

These equations may be solved directly by computer, but in the limit of small ω_2, a first-order perturbation result again has been obtained for v equivalent to Eq. 2 of Ref. 9. Just as one requires calculation of gain or loss in the Ω reference frame for the rotary field, the same is required for calculation of gain or loss at the frequency $\omega_l + \epsilon$ of the second laser beam.

B. Coupling between two traveling waves

In the limit of weak rotary perturbation, the gain or loss of the rotary field E_a as a traveling wave or as a standing wave may be obtained in terms of the intense laser field $\mathcal{E}_l$ which is assumed constant. Just as in stimulated Raman gain phenomena, one could as well allow these fields to couple arbitrarily and nonlinearly, but we will only show the linear coupling case here.

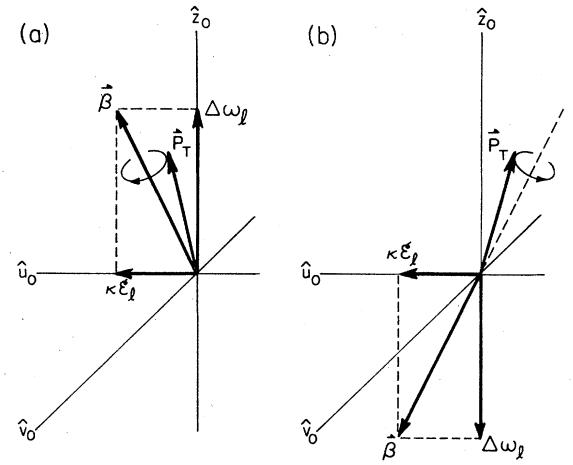

FIG. 7. Bloch vector diagrams of a two-level system (a) not inverted in the rotating frame ($\vec{P}_T \cdot \vec{\beta} > 0$) and (b) inverted in the rotating frame ($\vec{P}_T \cdot \vec{\beta} < 0$). Note that in neither (a) nor (b) is the population of the two-level system actually inverted.

Suppose Eq. (2) is specified as a traveling wave

$$E_a(z,t) = \tfrac{1}{2}\mathcal{E}_a(t) e^{i(\Omega t - kz)} + \text{c.c.} \tag{28}$$

The first-order terms given by Eqs. (21) in the rotating frame of the laser behave as independent Maxwell equation source terms for stimulated changes of $E_a(z,t)$ as a propagating rotary perturbation field at frequency Ω. Similarly, such changes would occur for $E_a(t)$ as a standing wave in a tuned cavity. Let $\Omega = \beta$ at exact rotary resonance, and by taking $\Omega T \gg 1$ and dropping terms with $(\Omega T)^{-4} \ll (\Omega T)^{-2}$, the term $v_{c,r}$ in Eq. (22) is therefore the principal source term. Under these conditions, the effects of dispersion can be neglected, (i.e., $u_{s,r} \ll v_{c,r}$). In the retarded time frame the slowly varying Maxwell equation[12] for the rotary field plane wave modulus in Eq. (28) is given by

$$\frac{d\mathcal{E}_a}{dz} = \frac{2\pi\Omega}{c} v_{c,r} = F\mathcal{E}_a\mathcal{E}_l\Delta\omega_l , \tag{29}$$

where

$$F = \frac{-\pi\Omega A(M_J)\kappa T^3}{c\hbar(1+\Omega^2T^2)} \tag{30}$$

is obtained from use of Eqs. (22c), (3), and (13). The saturating laser field is defined in first order by

$$\mathcal{E}_l(z) = \mathcal{E}_l(0) e^{-\alpha z} , \tag{31}$$

where $\alpha = 2Np_0\kappa^2\omega_l/c\mathcal{E}_l(0)$, and $\mathcal{E}_l(0)$ is the laser amplitude at $z = 0$. Equation (31) is applied to Eq. (29) which yields

$$\mathcal{E}_a(z) = \mathcal{E}_a(0)\exp[\alpha^{-1}F\mathcal{E}_l(0)\Delta\omega_l(1 - e^{-\alpha z})] .$$

The low-frequency field modulus $\mathcal{E}_a$ therefore undergoes a reduction or gain according to

$$\mathcal{E}_a(z \gg \alpha^{-1}) = \mathcal{E}_a(0)\exp[\alpha^{-1}|F|\mathcal{E}_1(0)\Delta\omega_1] ,$$

for $\alpha z \gg 1$, or $\mathcal{E}_a(z) = \mathcal{E}_a(0)\exp[zF\mathcal{E}_1(0)\Delta\omega_1]$ for $\alpha z \ll 1$, depending upon $\Delta\omega_1 = \pm|\Delta\omega_1|$. The choice of signs reflects which side of resonance the laser beam is applied. A complete analysis of the real physical case would require an integration over the inhomogeneous spectrum, i.e., Eq. (17), which would entail a competition between loss and gain because of simultaneous effects of terms with both signs above.

C. Rare optical dipole ↔ abundant spin double resonance coupling in a solid

The example of energy exchange between waves coupled to the optical two-level gaseous system above bears a similarity to the coupling among separate spin species carried out by double spin resonance experiments in solids.[6] With the condition of sufficiently long-lived optically excited states, it appears that a system of laser irradiated optical dipoles in dilute concentrations could be made to couple and exchange energy with neighboring spins in a solid. Consider the well known "solide effect" double resonance method[17,18] for obtaining polarized nuclei. The polarization of a nuclear spin reservoir is enhanced with positive or negative (inverted) orientation, determined by coupling with corresponding positive or negative orientations of electron spin neighbors strongly irradiated above or below resonance ($\pm\Delta\omega_1$), as viewed in the electron spin precession rotating frame. The optical rotary resonance coupling principle would be similarly operative in a solid where we now consider the optical system and the laser field $\mathcal{E}_1$ in place of the electron spins and the resonance microwave field, respectively. If the Larmor frequency ω_L of a foreign species of abundant spins is adjusted so that

$$\omega_L = \Omega = \beta , \tag{32}$$

the spins therefore can act as internal rotary perturbing field sources, analogous to E_a, and couple with the optical two-level system. The internal local field coupling may derive from magnetic dipolar or electric field interactions depending upon the nature of the optical two-level diagonal susceptibility.

In order to detect the transfer of energy between the two systems, one may monitor any measurable change in the character of the laser transmitted beam or a change in the spin population. This follows when conditions allow time for preparation of disparate two-level system "temperatures" or nonequilibrium population differences among level pairs. Therefore, at low temperatures optical systems with long lifetimes are required which have some character of a forbidden transition.

Without providing details here, we state below the necessary approximate relations among the essential double resonance parameters which would make the optical ion-spin system double resonance experiment feasible. The reader is referred to the double resonance literature for details and discussion.[6,18] Define R^{-1} as the resonance coupling time constant for equilibration of the dilute optical reservoir temperature with that of the spin system, and define $\epsilon \sim N_0/N_S \ll 1$ as the ratio of the quantum two-level heat capacity of the optical system to that of the spin system during resonance coupling, where N_0 and N_S are the optical ion and spin number density, respectively. Therefore $(\epsilon R)^{-1}$ is roughly the corresponding longer time constant for the spin system temperature change if the optical system is maintained away from its own equilibrium population or "heated" relative to the spin reservoir temperature. Since T is essentially the optical system fluorescence lifetime, this nonequilibrium heating is maintained if

$$T \lesssim R^{-1} . \tag{33}$$

However, the double resonance effect will have no resolution whatsoever and be washed out unless the condition $T \gg 2\pi/\omega_L$ applies, where $2\pi/\omega_L$ is the spin precession Larmor period. Also, T must not be too small with respect to the spin-spin coupling time T_{ss} and the time T_{s0} for a single photon exchange between an optical ion and its nearest neighbor. If it is too small the double resonance rate constant $R \sim (1/T_{s0}^2)[TT_{ss}/(T+T_{ss})]$ would then become ineffectively small. A change ΔM in spin polarization owing to the analogous coupling process in nuclear double resonance experiments[19] is given by

$$\Delta M(t) = M_0\exp(-t/T_{1s})\{1 - e^{-[\epsilon R/(1+RT)]t}\} ,$$

where T_{1s} is the spin lattice relaxation time. At time $t = 0$ the spin system is initially prepared at a different temperature from the lattice. The resonance coupling signified by $R \neq 0$ produces the $\Delta M(t)$ change in relaxation of the abundant spin species.

For arbitrary values of $\epsilon \sim N_0/N_S$, except for the restriction that N_0 must be small enough to avoid complications of direct coupling among the optical ions, the steady state polarizations which result from resonance coupling between the two systems can be estimated. Let the laser field $\mathcal{E}_1$ saturate the optical system at the exact resonance

condition $u = \Delta\omega_1 = 0$. The rotating frame temperature model predicts that an electric polarization $P = Np_0u'$ will build up (from $P \sim 0$) parallel to $\mathcal{E}_1$, if in addition the resonance condition $\omega_L = \kappa\mathcal{E}_1$ from Eq. (32) is satisfied. Therefore,

$$P = \epsilon M_0 R/(R + W_0).$$

Correspondingly, the equilibrium laboratory frame polarization M_0 of the spin system will diminish by an amount

$$\Delta M = M_0 Q/(1 + Q),$$

where

$$Q = \epsilon R W_0/(R + W_0)W_S, \quad W_S = T_{1S}^{-1},$$

and

$$W_0 = T^{-1}.$$

IV. CONCLUSIONS

The primary resonance character of single and multiphoton optical rotary saturation has been confirmed. The confirmation of predicted lineshapes by the experimental results is much less certain, and could be improved in future experiments which particularly take into account spatial variations in laser power over the excited regions of the gas sample. Because the semiclassical two-level descriptions in optics and spin resonance are essentially the same, it is not surprising that the optical rotary saturation effect can be added to a host of coherent optical two-level effects already found which are analogs of experiments in NMR. This effect can be classified as another type of nonlinear susceptibility where low-frequency radiation couples to a system which is at resonance with a high-frequency laser beam. Rotary saturation bears a strong similarity to the energy coupling which takes place between two waves tuned within the resonance line of an optical transition. Although the energy exchange between the coupled waves during optical rotary saturation is not demonstrated in this report, the analysis and mechanism of the coupling predicts a stimulated process of power transfer between the waves.

The direct solutions of nonlinear macroscopic Bloch equations for rotary saturation have been presented without the aid of "two-level temperature" arguments in the interaction representation used in the case of NMR in solids. The rotary resonance solutions are applicable to liquids or gases where the system is isolated except for the effects of macroscopic damping. The notion of "spin temperature" in a driven optical system is not generally applicable even in a solid, except possibly where the optical system is dilute and has an appropriately long fluorescence lifetime. In this circumstance, if the optical system couples by a cross-relaxation resonance process exclusively with another reservoir of two-level atoms (such as a spin system with an assigned spin temperature), the optical system may be described in terms of a temperature.

ACKNOWLEDGMENTS

We wish to thank Dr. R. G. Brewer of IBM, San Jose, for generously sharing with us the details of his Stark switching technique. One of us (E.L.H.) acknowledges the hospitality of the Max Planck Institute for Medical Research, Heidelberg, and the support of the Alexander von Humboldt Foundation during a portion of this work. This work was supported in part by the Division of Materials Research, National Science Foundation. This work was performed by one of us (Y.P.) in partial fulfillment of the requirements for the Ph.D. degree.

APPENDIX

In the usual perturbation approach we introduce a smallness parameter λ into Eqs. (6) by the substitution $\omega_a \to \lambda\omega_a$. Define $T_1 = T_2 = T$ and $\omega_1 = \kappa\mathcal{E}_1$. Solutions are assumed of the form

$$y = y_e + \lambda y_1 + \lambda^2 y_2 + \ldots + \lambda^n y_n + \ldots, \tag{A1}$$

where $y = u$, v, or w; $y_e = u_e$, v_e, or w_e; and $y - y_e$ corresponds to Δu, Δv, or Δw as defined in the text. After substitution of y into Eqs. (6) and collecting terms of the same order in λ^n, three differential equations result of the form

$$\dot{y} + a(t)y = b(t) \tag{A2}$$

for each n. For $\Delta u = \Delta v = \Delta w = 0$ at $t = 0$, the first-order ($n = 1$) corrections yield, from Eq. (A2),

$$u_1 = e^{-t/T}\int_0^t e^{t'/T}(2\omega_a \cos\Omega t' v_e + \Delta\omega_1 v_1)dt',$$

$$v_1 = -e^{-t/T}\int_0^t e^{t'/T}(2\omega_a \cos\Omega t' u_e + \Delta\omega_1 u_1 - \omega_1 w_1)dt', \tag{A3}$$

and

$$w_1 = -e^{-t/T}\int_0^t e^{t'/T}\omega_1 v_1 dt.$$

The coupled equations (A3) are combined by use of the following definitions:

$$M_1 = w_1' + iv_1.$$

$$w_1' = (-\omega_1 w_1 + \Delta\omega_1 u_1)\beta^{-1}, \tag{A4}$$

$$Z_1 = \Delta\omega_1\omega_a\beta^{-1}v_e - i\omega_a u_e,$$

and

$$\Gamma = T^{-1} + i\beta .$$

Applying these definitions to Eq. (A2) for $n=1$ yields the relation $\dot{M}_1 = 2Z\cos\Omega t - \Gamma M_1$, which has the solution

$$M_1(t) = Z_1 e^{-\Gamma t}\int_0^t [e^{(\Gamma+i\Omega)t'} + e^{(\Gamma-i\Omega)t'}]dt' \qquad \text{(A5)}$$

for $M_1(0)=0$. Transient solutions can be obtained from Eq. (A5), but here we present only the steady-state results. In steady state, $e^{-\Gamma t}\to 0$ with the result

$$M_1(t)_e = \frac{Z_1 e^{-i\Omega t}}{T^{-1} - i(\Omega-\beta)} + \frac{Z_1 e^{+i\Omega t}}{T^{-1} + i(\Omega+\beta)}$$

$$= M_{1,r}(t) + M_{1,ar}(t) ,$$

where (A6)

$$M_{1,r} = M_{1c,r}\cos\Omega t + M_{1s,r}\sin\Omega t ,$$

and

$$M_{1,ar} = M_{1c,ar}\cos\Omega t + M_{1s,ar}\sin\Omega t .$$

Resonant $(\Omega-\beta)$ and antiresonant $(\Omega+\beta)$ denominator terms are indicated by r and ar, respectively, and coefficients of cosine and sine terms are indicated by c and s, respectively.

The solution for v_1 is obtained as $v_1 = \mathrm{Im}\{M_1\}$. With v_1 substituted into expressions for $y=u_1$ and w_1 [Eq. (A3)] the solutions for u_1 and w_1 are obtained. In the text Eqs. (22) present the v_1 and u_1 resonant solutions, and the antiresonant solutions are obtained by the substitution $\Omega \to -\Omega$. Similarly, for $w_1(t)$ we have

$$w_1(t) = w_{1,r}(t) + w_{1,ar}(t) ,$$

$$w_{1,r}(t) = w_{1c,r}\cos\Omega t + w_{1s,r}\sin\Omega t ; \qquad \text{(A7)}$$

$$w_{1c,r} = \omega_1 T/(1+\Omega^2T^2)(v_{1c,r} - \Omega T v_{1s,r}) ,$$

$$w_{1s,r} = \omega_1 T/(1+\Omega^2T^2)(\Omega T v_{1c,r} + v_{1s,r}) .$$

The above procedure is repeated for obtaining higher-order corrections ($n>1$). For example, the next-order ($n=2$) terms, equivalent to Eq. (A4), would define $Z_2 = (\omega_a\Delta\omega_1/\beta)v_1 - i\omega_a u_1$. In contrast to Z_1, which is a constant, Z_2 has a time dependence of $\cos\Omega t$ and $\sin\Omega t$ from the v_1 and u_1 terms. The integration step in Eq. (A5) therefore results in the two photon rotary saturation resonant $(2\Omega-\beta)$ and antiresonant $(2\Omega+\beta)$ denominator terms. The nth correction therefore yields the nth multiphoton resonant condition $\Omega = \beta/n$. For example,

$$v_{2c,r} = \omega_a T\frac{-u_{1c} - (\beta-2\Omega)\Delta\omega_1\beta^{-1}Tv_{1c} + \Delta\omega_1\beta^{-1}v_{1s} - (\beta-2\Omega)Tu_{1s}}{2[1+(\beta-2\Omega)^2T^2]} . \qquad \text{(A8)}$$

*Present address: Gordon McKay Laboratory, 9 Oxford Street, Harvard University, Cambridge, Mass. 02138

[1]F. Bloch and A. Siegert, Phys. Rev. 57, 522 (1940).
[2]S. H. Autler and C. H. Townes, Phys. Rev. 78, 340A (1950).
[3]See a review by A. M. Bouch-Bonievich and V. A. Khodovoi, Usp. Fiz. Nauk. 93, 71 (1967) [Sov. Phys. Usp. 10, 637 (1968)].
[4]W. A. Anderson, Phys. Rev. 102, 151 (1956).
[5]A. G. Redfield, Phys. Rev. 98, 1787 (1955).
[6]S. R. Hartmann and E. L. Hahn, Phys. Rev. 128, 2042 (1962); F. M. Lurie and C. P. Slichter, Phys. Rev. 133, A1108 (1964); C. P. Slichter, *Principles of Magnetic Resonance*, Second edition (Springer-Verlag, New York, 1978), Chaps. VI and VII.
[7]Yehiam Prior and E. L. Hahn, Phys. Rev. Lett. 39, 1329 (1977).
[8]R. P. Feynman, F. L. Vernon, Jr., and R. W. Hellwarth, J. Appl. Phys. 28, 49 (1957).
[9]F. Y. Wu, S. Ezekiel, M. Ducloy, and B. R. Mollow, Phys. Rev. Lett. 38, 1077 (1977).
[10]Multiphoton rotary saturation transitions in NMR were observed by J. R. Franz and C. P. Slichter, Phys. Rev. 148, 287 (1966).
[11]R. G. Brewer and R. L. Shoemaker, Phys. Rev. Lett. 27, 631 (1971).
[12]See, for example, R. G. Brewer and E. L. Hahn, Phys. Rev. A 11, 1641 (1975).
[13]Because of the selection rule $\Delta M_J = 0$, either of the two oppositely precessing polarizations $P_+ = Np_0(u+iv)e^{+i\omega t}$ or $P_- = Np_0(u-iv)e^{-i\omega t}$ may be chosen in our description. The laboratory frame source polarization $P_+ + P_- = Np_0(u\cos\omega t - v\sin\omega t) = P_x$ is linearly polarized along x parallel to $E_x(z,t)$.
[14]S. B. Grossman, A. Schenzle, and R. G. Brewer, Phys. Rev. A 10, 2318 (1974).
[15]Yehiam Prior, Ph.D. dissertation, University of California, Berkeley (1977) (unpublished).
[16]The theoretical computer plot for multiphoton resonances in Fig. 2 of Ref. 7 was presented in error for the $+\Delta\omega_1$ instead of the $-\Delta\omega_1$ side of the $M_J=1$ line.
[17]A. Abragam, *The Principles of Nuclear Magnetism* (Oxford U. P., London, 1961), Chap. IX.
[18]Maurice Goldman, *Spin Temperature and Nuclear Magnetic Resonance in Solids* (Oxford U. P., London, 1970), Chap. VII.
[19]D. A. McArthur, E. L. Hahn, and R. E. Walstedt, Phys. Rev. 188, 609 (1969).